

Interactive Greybox Penetration Testing for Cloud Access Control using IAM Modeling and Deep Reinforcement Learning

YANG HU*, The University of Texas at Austin, USA

WENXI WANG*, The University of Texas at Austin, USA

SARFRAZ KHURSHID, The University of Texas at Austin, USA

MOHIT TIWARI, The University of Texas at Austin, USA

Identity and Access Management (IAM) is an access control service in cloud platforms. To securely manage cloud resources, customers need to configure IAM to specify the access control rules for their cloud organizations. However, incorrectly configured IAM can be exploited to cause a security attack such as privilege escalation (PE), leading to severe economic loss. To detect such PEs due to IAM misconfigurations, third-party cloud security services are commonly used. The state-of-the-art services apply whitebox penetration testing techniques, which require access to complete IAM configurations. However, the configurations can contain sensitive information. To prevent the disclosure of such information, customers need to manually anonymize the configuration.

In this paper, we propose a precise greybox penetration testing approach called TAC for third-party services to detect IAM PEs. To mitigate the dual challenges of labor-intensive anonymization and potentially sensitive information disclosures, TAC interacts with customers by selectively querying only the essential information needed. Our key insight is that only a small fraction of information in the IAM configuration is relevant to the IAM PE detection. We first propose IAM modeling, enabling TAC to detect a broad class of IAM PEs based on the partial information collected from queries. To improve the efficiency and applicability of TAC, we aim to minimize interactions with customers by applying Reinforcement Learning (RL) with Graph Neural Networks (GNNs), allowing TAC to learn to make as few queries as possible. Furthermore, to pretrain and evaluate TAC with enough diverse tasks, we propose an IAM PE task generator called IAMVulGen. Experimental results on both synthetic and real-world tasks show that, compared to state-of-the-art whitebox approaches, TAC detects IAM PEs with competitively low false negative rates, employing a limited number of queries.

1 INTRODUCTION

IAM [4] refers to an access control service in cloud platforms. It aims to securely manage the access to resources based on an IAM *configuration* specified by cloud customers with the access control rules in their cloud organizations. An IAM configuration consists of two components: entities (e.g., users and services such as Amazon EC2 instances) and permissions. Given a service request and an IAM configuration, IAM is able to check if the request obeys or violates the IAM configuration, and decide if the request should be allowed or denied.

Therefore, the correctness of IAM configurations plays an essential role in the effectiveness of cloud access control. Incorrect IAM configurations, namely IAM *misconfigurations*, can cause adverse security consequences such as data breaches, denial of services and resource hijacking [16, 39, 40, 43, 44], which have led to significant economic loss in recent years [37]. IAM PE [20, 28, 30] is an attack towards cloud access control that exploits the flaws within IAM to obtain additional permissions for performing sensitive operations or accessing sensitive data/resources. One of the most common ways to realize IAM PEs is to exploit IAM misconfigurations: the misconfigured IAM may allow the attacker to modify its configuration so that the attacker is allowed by the modified IAM configuration to obtain additional sensitive permissions.

*these authors contributed equally to this work.

Authors' addresses: Yang Hu, huyang@utexas.edu, The University of Texas at Austin, Austin, Texas, USA; Wenxi Wang, wenzix@utexas.edu, The University of Texas at Austin, Austin, Texas, USA; Sarfraz Khurshid, khurshid@ece.utexas.edu, The University of Texas at Austin, Austin, Texas, USA; Mohit Tiwari, tiwari@austin.utexas.edu, The University of Texas at Austin, Austin, Texas, USA.

To mitigate this issue, several cloud security services have been released to detect PEs due to IAM misconfigurations. There are two kinds of services: 1) *native* cloud security services [7–11] provided by cloud providers, and 2) *third-party* cloud security services provided [24, 26, 27] by cloud security startups, labs, open-source projects, etc. Native services usually aim to provide basic security guarantees for cloud customers, while third-party services aim to provide specialized security guarantees for cloud customers with complex and specialized demands [25, 52].

In this paper, we focus on third-party cloud security services for detecting PEs due to IAM misconfigurations. To our knowledge, all existing third-party services apply *whitebox* penetration testing techniques [21, 23, 33, 34, 47, 53], which require the access to complete IAM configurations. However, sharing the entire IAM configurations to third-party cloud security services can raise a potential security risk in leaking sensitive information of their cloud organizations (e.g., the internal organization architecture). This level of transparency might not be acceptable for cloud customers in fields with elevated security requirements, such as healthcare, finance, and government [31, 41, 46]. To mitigate the security concerns, cloud customers have to anonymize the sensitive information in their IAM configurations before using third-party services, which could take a significant amount of manual efforts. Moreover, the labor-intensive anonymization leads to a significant shortage of publicly available real-world IAM configurations, which impedes academic and open research communities from engaging effectively in addressing the issue.

To avoid both laborious anonymizations and sensitive information disclosure, we propose a precise greybox penetration testing approach called TAC to detect IAM PEs. The idea is to intelligently interact with cloud customers by a sequence of queries, requesting only the essential information needed for the detection. Specifically, each query seeks information about one permission assignment (i.e., whether a particular permission is assigned to a specific entity). During each interaction, customers will be presented with one query and given the option to either accept or decline the query based on their knowledge of whether the query might potentially result in the exposure of confidential information. In addition, customers are allowed to set up a query budget, which is the maximum number of queries they are willing to interact with. The primary goal of TAC is to detect the IAM PE within the query budget. Furthermore, to make TAC practically applicable, the main challenge lies in minimizing customer inputs, thereby reducing the total number of queries during the detection process.

To achieve the goal and overcome the challenge, TAC faces two problems: 1) detecting PEs based on partial information of IAM configurations collected by queries, and 2) learning to generate as few queries as possible to perform the detection within the query budget. To solve the first problem, we propose a comprehensive IAM modeling, for detecting a broader class of PEs than the existing whitebox detectors. In particular, to detect PE only with partial information, we propose abstract modeling for IAM configurations based on our *Permission Flow Graph* (PFG) with predefined abstract states and rules for updating the configuration with partial information provided by the queries. For the second problem, we formulate it into an RL problem, and apply GNN-based deep RL with pretraining to solve the problem.

Pretraining and evaluating TAC require a large number of diverse tasks. To our knowledge, there is only one publicly available IAM PE task set called IAM `Vulnerable` [1] containing only 31 tasks. Regarding this, we propose an IAM PE task generator called IAMVulGen which randomly generates IAM PE tasks from a large entity and permission space with diverse types manually identified from Amazon Web Services (AWS) official documentation [4–6] and studies on IAM PEs [20, 28, 30, 60].

To evaluate TAC, we used 500 tasks generated by IAMVulGen, the 31 tasks from the only publicly available IAM PE task set IAM `Vulnerable`, and two real-world IAM PE tasks collected from a U.S. based security startup as our evaluation benchmarks. For baselines, since there is no existing greybox or blackbox penetration testing tool regarding IAM PEs, we take three state-of-the-art

whitebox penetration testing tools, namely Pacu [33], Cloudsplaining [47] and PMapper [21] as our baselines. In addition, to understand how our IAM modeling contributes to TAC, we build a whitebox variant of TAC that solely applies our IAM modeling to detect PEs. To assess how our proposed GNN-based RL with pretraining enhances TAC, we build three greybox variants of TAC, each of which employs a different pretraining strategy or query model.

As a result, on the synthesized IAM PE task set by IAMVulGen, TAC’s whitebox variant successfully detected all PEs, and significantly outperforms all three state-of-the-art whitebox baselines, showing the outstanding effectiveness of our IAM modeling. In addition, given a query budget of 100, TAC identifies 6% to 38% more PEs with 16% to 23% fewer queries on average than all its three greybox variants, demonstrating the superiority of our pretraining based deep RL approach. On the only publicly available task set IAM Vulnerable [1], TAC is able to detect 23 PEs under a query budget of 10, and all 31 PEs with a query budget of 20, which substantially outperforms all three whitebox baselines. Furthermore, TAC successfully detects two real-world PEs with a query budget of 60. The contributions of this paper are:

- **Modeling.** A comprehensive modeling for IAM configurations is introduced, providing the foundation of IAM PE detection.
- **Approach.** TAC is the first interactive greybox penetration testing tool for third-party cloud security services to detect PEs due to IAM misconfigurations.
- **Synthetic Data.** An IAM PE task generator called IAMVulGen is proposed.

2 BACKGROUND

2.1 RL Basics

RL refers to a set of algorithms that aim to learn to make decisions from interactions [57]. An RL problem is usually formulated as a Markov Decision Process (MDP). In MDP, the learner or the decision maker is called the *RL agent*. The RL agent interacts with the *environment* which maintains its internal *state*. In each interaction between the RL agent and the environment, the RL agent chooses an *action* to perform; the environment then updates its *state* based on the action, and returns a *reward* quantifying the effectiveness of the action.

In this paper, we only consider a finite sequence of interactions between the RL agent and the environment, which are divided into several sub-sequences, namely *episodes*. Each episode starts from an *initial state* and ends with a *terminal state*. If an episode ends, the state of the environment will be automatically reset to the initial state for the next episode to start. The *return* refers to the cumulative rewards for one episode. The goal of the RL agent is to learn an *RL policy* for choosing an action per interaction that maximizes the expected return.

2.2 IAM Basics

2.2.1 IAM Configurations. IAM configuration consists of two components: entities and permissions. An entity represents either a subject or a role in an IAM configuration. Subjects (i.e., users, user groups and services) can actively perform actions. Roles are created to represent job functions and responsibilities within an organization. Permissions refer to privileges of performing operations. An entity in an IAM configuration can obtain permissions in both direct and indirect ways. Permissions can be directly assigned to users, user groups and roles; permissions assigned to an entity can be *indirectly* assigned to another entity in many ways, depending on the relationship between the two entities. For example, all permissions assigned to a user group can be indirectly assigned to a user in the user group; all permissions assigned to a role can be indirectly assigned to a user who assumes the role (i.e., become a member of the role).

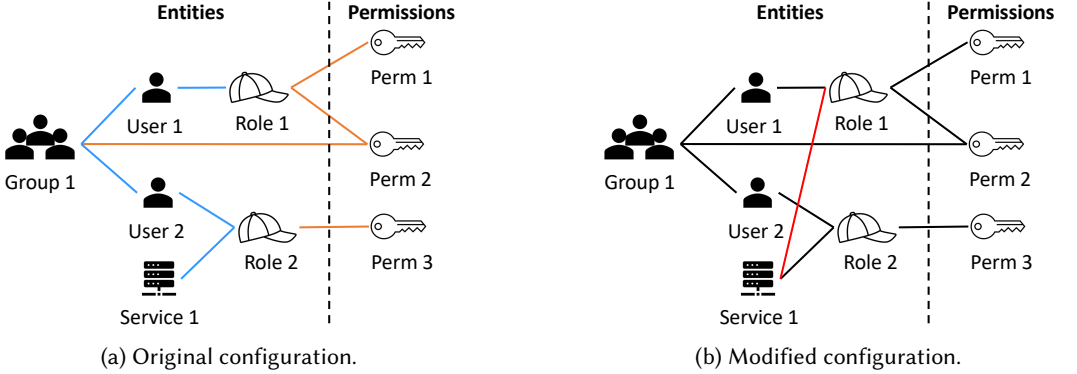


Fig. 1. An illustrative example of a PE due to IAM misconfiguration, derived from a notable real-world incident in 2019. Figure (a) shows the original IAM configuration, where the entity-entity and entity-permission connections are highlighted in blue and orange, respectively. Figure (b) shows the modified IAM configuration in the PE, where the modification is highlighted in red.

Figure 1a presents an IAM configuration example as a relational graph. In the example, there are six entities with four entity types: one user group Group 1, two users User 1 and User 2, one service Service 1, and two roles Role 1 and Role 2. Besides, there are three permissions: Perm 1, Perm 2 and Perm 3. Each entity-permission connection denotes that the permission is directly assigned to an entity. In the example, Perm 1 and Perm 2 are directly assigned to Role 1; Perm 2 is directly assigned to Group 1; Perm 3 is directly assigned to Role 2. Each entity-entity connection denotes that one entity is currently related to another under the relation between their entity types. In the example, there are five entity-entity connections under three relations: user-group relation representing that a user is in a user group, user-role relation representing that a user assumes a role, and service-role relation representing that a service assumes a role. Based on the semantics of the user-group relation illustrated above, User 1 and User 2 in Group 1 can indirectly obtain the permission Perm 2 directly assigned to the group. Similarly, based on the semantics of user-role and service-role relations, both User 2 and Service 1 obtain Perm 3 indirectly by assuming Role 2.

2.2.2 PEs due to Misconfigurations. The PE on IAM [20, 28, 30] is the act of exploiting the IAM’s flaws to obtain additional permissions for performing the sensitive operation or accessing sensitive data/resources. One of the most common causes of PEs is due to IAM *misconfigurations*, which is the main focus in this paper. The misconfigured IAM may allow the attacker to change its configuration so that the attacker is allowed by the modified IAM configuration to obtain additional sensitive permission. We define the *untrusted entity* as the entity controlled by the attacker, and the *target permission* as the permission that the attacker targets to obtain illegally. The attacker realizes a PE by controlling the untrusted entity to modify the IAM misconfiguration such that the target permission is assigned to the untrusted entity.

For illustration purposes, we craft a simplified version of a notorious real-world IAM PE in 2019 [29, 40], which gained access to 100 million credit card applications and accounts in Capital One bank. Our illustrative example is shown in Figure 1. In the real-world PE example, the untrusted entity is an Amazon EC2 instance; the target permission is a permission allowing to access a sensitive S3 bucket, which contains customers’ credit card application data. In our illustrative example, Service 1 corresponds to the untrusted entity, Perm 1 corresponds to the target permission, and

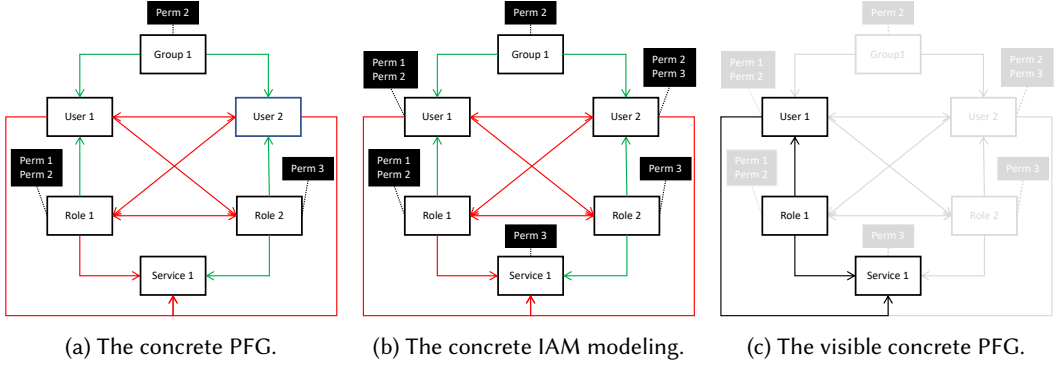


Fig. 2. PFGs of the illustrative example shown in Figure 1a. Permission flows with enabled states are annotated in green; with disabled states are annotated in red; with unknown states are annotated in black.

Perm 3 allows the untrusted entity to assume Role 1. During the PE as shown in Figure 1, the attacker controls the untrusted entity to obtain the target permission in two steps: 1) the untrusted entity Service 1 indirectly obtains Perm 3 by assuming Role 2; 2) the untrusted entity Service 1 applies Perm 3 to assume Role 1, and thus indirectly obtains the target permission Perm 1 from Role 1.

The example above illustrates a *single-step* PE, where the untrusted entity uses one permission to realize PE. However, a more complicated *multi-step* PE (or *transitive* PE) [23, 53] can occur, involving multiple permissions. This paper focuses on detecting both PE types.

3 IAM MODELING

We present our *concrete IAM modeling* using the proposed *Permission Flow Graph*. We further propose our *abstract IAM modeling*, which provides the foundation of our greybox penetration testing approach.

3.1 Concrete IAM Modeling

3.1.1 The Permission Flow. We first propose the *permission flow* to model an indirect permission assignment from one entity to another. Each permission flow has a *flow state* representing whether the flow is currently enabled or disabled. If a permission flow from entity e_1 to entity e_2 is currently enabled, all permissions assigned to e_1 can be automatically assigned to e_2 ; otherwise (i.e., the permission flow is currently disabled), the permissions cannot be automatically assigned.

Whether there is a permission flow between two entities depends on whether there exists a relation between the two entity types whose semantics are associated with indirect permission assignments. For example, based on the semantics of the user-role relation stating that all permissions assigned to a role can be indirectly assigned to the user who assumes the role, there exists a permission flow from each role entity to each user entity. Accordingly, there exist four permission flows from Role 1 / Role 2 to User 1 / User 2 in the illustrative IAM configuration example shown in Figure 1a. The permission flows can be manually extracted based on the semantics of entity-entity relations from AWS documentation and relevant studies[5, 20, 28, 30, 60]. Details about identifying permission flows is introduced in Section 6.

The state of each permission flow is determined by the relationship between the two entities involved in the flow. If they are currently related, the flow state is marked as enabled. Otherwise, it is marked as disabled. An illustration of this can be found in Figure 1a (showing the illustrative

IAM configuration example) and Figure 2a (showing its corresponding permission flow states). In Figure 1a, User 1 is related to Role 1 but unrelated to Role 2; in alignment with this, in Figure 2a, the flow from Role 1 to User 1 is enabled, whereas the flow from Role 2 to User 1 is disabled.

3.1.2 The Permission Space. Next, we introduce the permission space considered in our concrete modeling. We identify two types of permissions which can be utilized by the untrusted entity to obtain the target permission. We call them Type-I and Type-II permissions. A Type-I permission allows to enable a permission flow from one entity e_1 to another entity e_2 such that all permissions of e_1 are automatically assigned to e_2 . A Type-II permission allows to directly assign a Type-I or target permission (denoted as p) to an entity e . For example, the permission for adding a user to a user group is a Type-I permission. The permission for attaching an IAM policy to a user is a Type-II permission, as it directly assigns each permission in the policy to the user.

The permission space in our modeling consists of all Type-I permissions (denoted as P_I), all Type-II permissions (denoted as P_{II}) and the target permission (if the target permission is neither the Type-I nor Type-II permission). Figure 1a shows three permissions in the permission space: Perm 1, Perm 2, and Perm 3. Perm 1 is the target permission. Perm 2 is the Type-II permission which allows its assigned entity to directly assign the target permission Perm 1 to Role 1. Perm 3 is the Type-I permission which allows its assigned entity to assume Role 1, that is enabling a permission flow from the assigned entity to Role 1.

3.1.3 The PFG. We propose the PFG to concretely model an IAM configuration. A PFG includes entities as its nodes and permission flows as its edges. Formally, a PFG is defined as a tuple $G = (E, F, \mathcal{A}, \mathcal{W})$, where E denotes the entity space; $F \subseteq E \times E$ denotes a set of permission flows; $\mathcal{A} : E \mapsto 2^P$ denotes a permission assignment function which maps an entity to permissions in the permission space P ; $\mathcal{W} : F \mapsto \{\text{true}, \text{false}\}$ denotes a concrete flow state function which outputs whether a permission flow is currently enabled (denoted as true) or disabled (denoted as false). Figure 2a shows a PFG which straightforwardly models the IAM configuration example shown in Figure 1a. Three entities (i.e., Group 1, Role 1 and Role 2) are directly assigned with permissions. According to the semantics of user-role relation, service-role relation and user-group relation which are all associated with indirect permission assignments, there are 12 identified permission flows between the entities with the corresponding entity types. As shown in Figure 1a, five of the entity-entity pairs are currently related, thus resulting in five enabled permission flows. The remaining seven flows are disabled.

3.1.4 Concrete Modeling of IAM Configurations. Given a PFG $G = (E, F, \mathcal{A}, \mathcal{W})$, we define the permission flow function returning a new PFG $G' = (E, F, \mathcal{A}', \mathcal{W})$ by performing one permission flow iteration. The permission flow function \mathcal{M} is defined as $G' = \mathcal{M}(G)$ where

$$\mathcal{A}'(e_2) = \bigcup_{\{(e_1, e_2) \in F \mid \mathcal{W}(e_1, e_2) = \text{true}\}} \mathcal{A}(e_1) \cup \mathcal{A}(e_2)$$

meaning that, for each entity e_2 , all permissions of the entities which have enabled permission flows to e_2 are assigned to e_2 .

Given a PFG G , we perform the fixed point iteration w.r.t. the permission flow function \mathcal{M} on G . The resulting PFG denoted as G' is our concrete model of the IAM configuration. Formally, $G' = \mathcal{M}^*(G)$, where \mathcal{M}^* refers to the fixed point iteration of \mathcal{M} (i.e., $\mathcal{M}^*(G) = \mathcal{M}^n(G)$ s.t. $\mathcal{M}^n(G) = \mathcal{M}^{n-1}(G)$). Figure 2b shows a concrete modeling of the illustrative IAM configuration example shown in Figure 1a, which is the fixed point of the PFG in Figure 2a. Based on five enabled permission flows, the PFG is updated with indirect permission assignments: User 1 and User 2 indirectly obtain Perm 2 from Group 1; User 2 and Service 1 indirectly obtain Perm 3 from

Role 2; User 1 indirectly obtains Perm 1 and Perm 2 from Role 1. The resulting PFG can no longer be updated further by any indirect permission assignments, having reached a fixed point.

3.1.5 Concrete Modeling of IAM PEs. An IAM configuration has a PE iff the untrusted entity can obtain the target permission through the permissions assigned to the untrusted entity. Formally, let $G_0 = (E_0, F_0, \mathcal{A}_0, \mathcal{W}_0)$ be an initial IAM configuration, u be the untrusted entity, and $l \in P \setminus \mathcal{A}_0(u)$ be a target permission; the concrete IAM configuration G_0 has a PE iff there exists a sequence of permissions p_1, \dots, p_n , where $p_i \in \mathcal{A}_{i-1}(u)$, and a modified IAM configuration $G_n = (E_n, F_n, \mathcal{A}_n, \mathcal{W}_n)$ such that

$$G_0 \xrightarrow{p_1} G_1 \dots \xrightarrow{p_n} G_n \wedge l \in \mathcal{A}_n(u),$$

where $G_{i-1} \xrightarrow{p_i} G_i$ annotates that the concrete IAM configuration G_{i-1} is modified to G_i by the untrusted entity u through the permission $p_i \in \mathcal{A}_{i-1}(u)$.

3.2 Abstract IAM Modeling

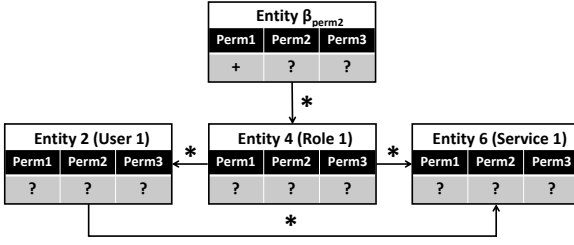
The above concrete IAM modeling requires full access to the IAM configuration. However, not all permission assignment information in the IAM configuration is necessary for detecting PEs. For instance, the PE shown in Figure 1b can be detected using only the following partial permission assignment information: Service 1 owns Perm 3, and Role 1 owns Perm 1. Based on this insight, we propose our abstract IAM modeling that can identify PEs using partial permission assignment information, forming the foundation of our greybox penetration testing technique.

3.2.1 Abstract PFG. The abstract PFG aims to model the IAM configurations with partially *visible entities* and the permission flows among them with unknown flow states (which are called *visible permission flows*). For the illustrative example, the visible entities User 1, Role 1 and Service 1; and the visible permission flows are shown in Figure 2c. With the visible entity space $E_{\text{vis}} \subseteq E$ and the visible permission flow space $F_{\text{vis}} \subseteq F$, we construct a visible permission space $P_{\text{vis}} \subseteq P$ which only includes Type-I and Type-II permissions that are related to E_{vis} or F_{vis} (i.e., permissions which can directly assign a permission to a visible entity or enable a visible permission flow), and the target permission. Given the visible entities, visible permission flows and visible permissions, we define our abstract PFG as a tuple $\hat{G} = (\hat{E}, \hat{F}, \hat{\mathcal{A}}, \hat{\mathcal{W}})$, where \hat{E} denotes the abstract entity space; \hat{F} denotes the abstract permission flow space; $\hat{\mathcal{A}}$ denotes the abstract entity-permission state function; $\hat{\mathcal{W}}$ denotes the abstract permission flow state function. In the following, we elaborate each of these components in detail.

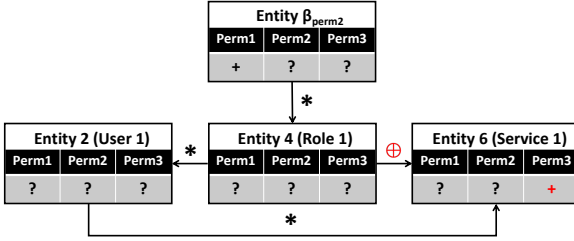
In the construction of our abstract entity space and permission flow space, the initial step involves transforming each Type-II permission into a Type-I permission. This transformation step aims to simplify the formulation of state transitions which will be demonstrated later in this section. Recall that a Type-II permission s , if being assigned to an entity, allows the entity to directly assign a target permission or a Type-I permission t_s to an entity e_s . For each Type-II permission s , we 1) add a *pseudo entity* β_s assigned with the corresponding target or Type-I permission t_s , and 2) add the *pseudo permission flow* from the pseudo entity β_s to the corresponding entity e_s . This way, each Type-II permission s becomes a Type-I permission which allows the assigned entity to enable the pseudo permission flow from the pseudo entity β_s to the corresponding entity e_s . With the transformations, we then define our abstract entity space \hat{E} and abstract flow space \hat{F} by extending the visible entity space E_{vis} and the visible flow space F_{vis} , with the pseudo entities and pseudo permission flows, respectively. Formally, $\hat{E} = E_{\text{vis}} \cup \{\beta_s | s \in P_{\text{II}} \cap P_{\text{vis}} \wedge e_s \in E_{\text{vis}}\}$, and $\hat{F} = F_{\text{vis}} \cup \{(\beta_s, e_s) | s \in P_{\text{II}} \cap P_{\text{vis}} \wedge e_s \in E_{\text{vis}}\}$.

Next we define our abstract entity-permission state function $\hat{\mathcal{A}} : \hat{E} \times P_{\text{vis}} \mapsto \{?, +\}$ maps each entity-permission pair to an abstract state. $\hat{\mathcal{A}}(e, p) = ?$ means that it is unknown whether the permission p can be assigned to the entity e or not; $\hat{\mathcal{A}}(e, p) = +$ means that the permission p can be assigned to the entity e , either directly or indirectly. Initially, the entity-permission state function assigns $?$ to all entity-permission pairs except for the pairs of each pseudo entity and the corresponding Type-I or target permission (involved in the Type-II permission). Formally, the initial abstract entity-permission state function $\hat{\mathcal{A}}_{\text{init}}(e, p)$ is defined as

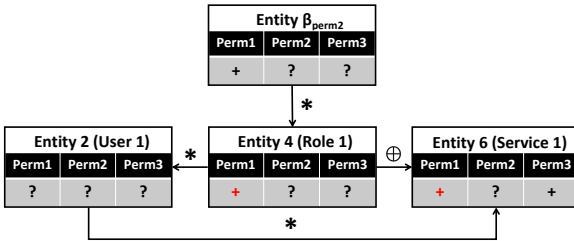
$$\hat{\mathcal{A}}_{\text{init}}(e, p) = \begin{cases} +, & \exists s \in P_{\text{II}} \cap P_{\text{vis}}, e = \beta_s \wedge p = t_s, \\ ?, & \text{otherwise.} \end{cases}$$



(a) The initial abstract IAM configuration representing the visible concrete PFG in Figure 2c.



(b) The intermediate abstract configuration updated with the response $\mathcal{O}(\text{Entity 6, Perm 3})$.



(c) The terminal abstract IAM configuration updated with the response $\mathcal{O}(\text{Entity 4, Perm 1})$.

Fig. 3. An illustrative example introducing our interactive greybox penetration testing approach for IAM PEs; for demonstration purposes, we only show three visible permissions.

The abstract permission flow state function $\hat{\mathcal{W}} : \hat{F} \mapsto \{*, \oplus\}$ maps each permission flow to an abstract state. $\hat{\mathcal{W}}(f) = *$ means that it is unknown whether the permission flow f can be enabled or not; $\hat{\mathcal{W}}(f) = \oplus$ means that the permission flow can be enabled. Initially, the states of all permission flows are mapped to $*$, which is defined as $\forall f \in \hat{F}. \hat{\mathcal{W}}_{\text{init}}(f) = *$.

Figure 3a shows an example of an initial abstract PFG $\hat{G}_{\text{init}} = (\hat{E}, \hat{F}, \hat{\mathcal{A}}_{\text{init}}, \hat{\mathcal{W}}_{\text{init}})$, which is the abstract modeling of the visible concrete PFG example shown in Figure 2c. Recall that Perm 2 is the Type-II permission which allows its assigned entity to directly assign the target permission Perm 1 to Role 1. Perm 2 is converted into a Type-I permission with the added pseudo permission flow from the pseudo entity Entity β_{perm2} to Role 1. The abstract entity space is expanded with the added pseudo entity Entity β_{perm2} . The abstract permission flow space is also expanded with the added pseudo permission flows. The entity-permission states are initialized to $?$, except for the state of the pseudo entity Entity β_{perm2} and the target permission Perm 1 (involved in the Type-II permission Perm 2) being initialized to $+$. All permission flow states are initialized to $*$.

3.2.2 Abstract Permission Flow Function. Given an abstract PFG $\hat{G} = (\hat{E}, \hat{F}, \hat{\mathcal{A}}, \hat{\mathcal{W}})$, the abstract permission

flow function \hat{M} outputs a new PFG $\hat{G}' = (\hat{E}, \hat{F}, \hat{\mathcal{A}}', \hat{\mathcal{W}}')$ by performing one permission flow iteration. Formally, the function is defined as $\hat{G}' = \hat{M}(\hat{G})$, where

$$\hat{\mathcal{A}}'(e, p) = \begin{cases} +, & \mathbf{C1}: \exists e' \in N_{\oplus}^{(e)}. \hat{\mathcal{A}}(e', p) = +, \\ \hat{\mathcal{A}}(e), & \text{otherwise.} \end{cases}$$

$$\hat{\mathcal{W}}'(f) = \begin{cases} \oplus, & \mathbf{C2}: \exists p \in P_I \cap P_{\text{vis}}. \llbracket p \rrbracket = f \wedge \hat{\mathcal{A}}(u, p) = +, \\ \hat{\mathcal{W}}(f), & \text{otherwise.} \end{cases}$$

Here, $N_{\oplus}^{(e)} = \{e' \mid (e', e) \in \hat{F} \wedge \hat{\mathcal{W}}(e', e) = \oplus\}$; $\llbracket p \rrbracket$ refers to the permission flow that can be enabled with the Type-I permission p .

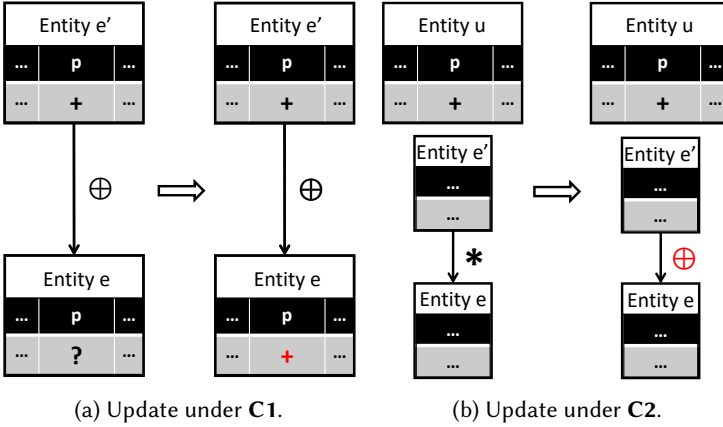


Fig. 4. Abstract state updates.

The condition **C1** is used to update the abstract state of an entity-permission pair. If there exists an entity e' having the permission p (i.e., the abstract state is $+$) and an enabled permission flow (i.e., the permission flow state is \oplus) from the entity e' to an entity e , then e can have the permission p (i.e., the abstract state of the pair (e, p) is updated to $+$). Figure 4a illustrates how the abstract state of an entity-permission pair gets updated under the condition **C1**.

The condition **C2** is used to update the abstract state of a permission flow. If there exists a permission p assigned to the compromised entity u (i.e., the abstract state of the pair (u, p) is $+$) and the permission p is a Type-I permission which allows to enable a permission flow f , then the permission flow f can be enabled (i.e., the abstract state of f is updated to \oplus). Figure 4b illustrates how the abstract state of a permission flow gets updated under condition **C2**.

3.2.3 Abstract IAM Configuration Modeling. Similar with the concrete IAM configuration modeling, given an abstract PFG \hat{G} , we perform the fixed point iteration w.r.t. the abstract permission flow function \hat{M} on \hat{G} . The resulting \hat{G}' is our abstract model of the IAM configuration. Formally, $\hat{G}' = \hat{M}^*(\hat{G})$ where \hat{M}^* refers to the fixed point iteration of \hat{M} (i.e., $\hat{M}^*(G) = \hat{M}^n(G)$ such that $\hat{M}^n(G) = \hat{M}^{n-1}(G)$).

In particular, the initial abstract PFG $\hat{G}_{init} = (\hat{E}, \hat{F}, \hat{\mathcal{A}}_{init}, \hat{\mathcal{W}}_{init})$ (introduced in Section 3.2.1) is the initial abstract IAM configuration. In addition, $\hat{G}_{term} = (\hat{E}, \hat{F}, \hat{\mathcal{A}}_{term}, \hat{\mathcal{W}}_{term})$ denotes the *terminal* abstract IAM configuration, where $\hat{\mathcal{A}}_{term}(u, l) = +$. The rest configurations are referred to as *intermediate* abstract IAM configurations. Figure 3 shows three abstract IAM configurations abstracting the partially visible PFG shown in Figure 2c, including an initial abstract configuration

(Figure 3a), an intermediate abstract configuration (Figure 3b) and a terminal abstract configuration (Figure 3c).

4 TAC

4.1 Overview

Based on abstract IAM modeling, we propose a greybox penetration testing approach called TAC for detecting IAM PEs, without requiring a complete IAM configuration. Unlike existing whitebox penetration testing approaches which force their customers to pay lots of manual efforts to blindly eliminate all sensitive information of their IAM configurations, TAC actively interacts with cloud customers to query only the essential information related to PE detection.

TAC only requires cloud customers to provide two simple initial inputs beforehand: 1) the type of the untrusted entity and the target permission; 2) the types of visible entities that they are inclined to be queried with. TAC renames each visible entity (including the untrusted entity) with a randomly generated entity ID; constructs the visible permissions with the renamed visible entities; and creates visible permission flows (with unknown flow states) among visible entities based on their types. These visible entities, visible permissions, and visible permission flows are used to create the initial abstract IAM configuration. For the illustrative example, suppose the customer chooses User 1, Role 1 and Service 1 as the visible entities, they are randomly renamed by TAC as Entity 2, Entity 4, and Entity 6, respectively. The converted initial abstract IAM configuration is shown in Figure 3a.

TAC delivers one query to the cloud customer at a time, inquiring whether a visible permission is assigned to a visible entity. The cloud customer can choose to either respond to or decline the query, based on their knowledge of whether the inquired permission assignment information is confidential. Formally, let $Q = E_{\text{vis}} \times P_{\text{vis}}$ be the query space. The response of the cloud customer w.r.t. a concrete IAM configuration $G = (E, F, \mathcal{A}, \mathcal{W})$ is defined as a function $O : Q \mapsto \{\text{true}, \text{false}, \text{unknown}\}$ satisfying

$$O(e, p) = \begin{cases} \text{true}, & \text{accept} \wedge p \in \mathcal{A}(e), \\ \text{false}, & \text{accept} \wedge p \notin \mathcal{A}(e), \\ \text{unknown}, & \neg \text{accept} \end{cases}$$

where the boolean variable *accept* denotes whether the customer accepts to answer the query.

Additionally, TAC allows cloud customers to specify the number of queries they accept to response, which is called the *query budget*. TAC outputs if a PE is detected within the query budget. In TAC, an IAM configuration has a PE iff its initial abstract configuration can be updated to a terminal abstract configuration, based on the customer query responses. Formally, let $\hat{G}_0 = (\hat{E}_0, \hat{F}_0, \hat{\mathcal{A}}_0, \hat{\mathcal{W}}_0)$ be an initial abstract IAM configuration, u be the untrusted entity, and l be the target permission. The initial abstract IAM configuration \hat{G}_0 has an abstract PE iff there exists a sequence of queries $(e_1, p_1), \dots, (e_n, p_n) \in Q$, and a terminal abstract IAM configuration $\hat{G}_n = (\hat{E}_n, \hat{F}_n, \hat{\mathcal{A}}_n, \hat{\mathcal{W}}_n)$ such that

$$\hat{G}_0 \xrightarrow{(e_1, p_1)} \hat{G}_1 \dots \xrightarrow{(e_n, p_n)} \hat{G}_n \wedge \hat{\mathcal{A}}_n(u, l) = +,$$

where $\hat{G}_{i-1} \xrightarrow{(e_i, p_i)} \hat{G}_i$ annotates that the abstract IAM configuration \hat{G}_{i-1} is updated to \hat{G}_i based on the customer response of the query (e_i, p_i) :

$$\hat{G}_i = \begin{cases} \hat{M}^*(\hat{G}_{i-1}[\hat{\mathcal{A}}_{i-1}[e_i, p_i] \mapsto +]), & O(e_i, p_i) = \text{true}, \\ \hat{G}_{i-1}, & \text{otherwise.} \end{cases}$$

Note that our abstract IAM modeling and state updating rules guarantee the precision of IAM PE detection, meaning that the PE identified by TAC must be a true PE.

We use the illustrative example (shown in Figure 3) to briefly introduce how TAC interacts with its customer through queries to detect IAM PEs. Given the initial abstract IAM configuration in Figure 3a, TAC may query the customer whether Entity 6 initially has the permission Perm 3 (i.e., the query (Entity 6, Perm 3)). The customer answers yes to the query (i.e., $O(\text{Entity 6, Perm 3}) = \text{true}$). Thus, the abstract state of the entity-permission pair (Entity 6, Perm 3) is updated to +. In addition, Perm 3 is the Type-I permission which allows its assigned entity (i.e., Entity 6) to enable the permission flow from Entity 4 to Entity 6. Thus, the abstract state of the permission flow from Entity 4 to Entity 6 is updated to \oplus . The resulting intermediate abstract IAM configuration is shown in Figure 3b. Next, TAC may send another query to see whether Entity 4 has the target permission Perm 1 (i.e., the query (Entity 4, Perm 1)). As a result, the customer answers yes to the query (i.e., $O(\text{Entity 4, Perm 1}) = \text{true}$). Thus, the abstract state of the entity-permission pair (Entity 4, Perm 1) is updated to +. Based on the condition C1 of the abstract permission flow function \hat{M} , the abstract state of the entity-permission pair (Entity 6, Perm 1) is updated to +. Since the initial IAM configuration can be updated to the terminal abstract IAM configuration shown in Figure 3c, the initial configuration has a PE.

4.2 General Framework

To be practically applicable, TAC aims to minimize the customer responses. To achieve this, the goal is to detect the IAM PE with as few queries as possible within the query budget. The problem is a *sequential decision making* problem, where each query is selected based on the customer's responses of previous queries. To solve the problem, we apply RL to learn to use as few queries as possible to identify the IAM PEs. The general framework of TAC is designed based on our RL formulation of the problem, as shown in Figure 5.

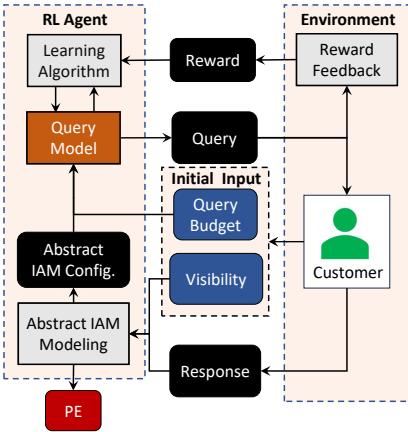


Fig. 5. The general framework of TAC.

In each episode, the RL agent begins with its visibility, an initial abstract IAM configuration, and a query budget. The agent iteratively sends queries to update the abstract IAM configuration until either a PE is identified or the query budget is exhausted. In each iteration, an RL agent uses a *query model* (i.e., the RL policy) for selecting one query (i.e., the action) based on the current abstract IAM configuration (i.e., the state). In the environment of our RL formulation, the abstract IAM configuration is updated based on the customer response of the query; a reward, which is -1 for each query, is output by a reward feedback module. The RL agent then uses the classic Actor-Critic Method [57] as the learning algorithm to update the query model based on the reward. Note that the current rewards and future rewards are treated equally important (i.e., the reward discount factor is set to 1). The goal of the RL agent is to learn a good query model to maximize the return, which is equivalent to minimizing the number of queries.

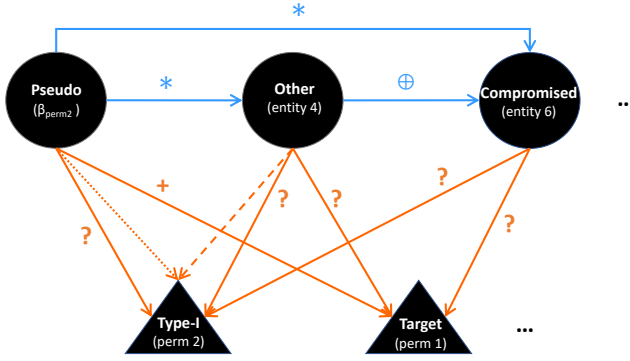


Fig. 6. The graph representation of the abstract IAM configuration in Figure 3b for GNN (Entity 2 and Perm 3 are omitted). Each entity node is represented with a circle; each permission node is represented with a triangle; each entity-entity edge representing a permission flow is annotated in a blue line and each entity-permission edge is annotated in an orange line (an edge representing a permission assignment is represented in a solid line; an edge from a source/sink entity of the permission flow in a Type-I permission to the corresponding Type-I permission is represented in a dotted/dashed line, respectively).

Note that the formulated RL problem requires the RL agent to detect the PE within only one episode. However, classic deep RL approaches [57] usually train an RL policy from scratch (i.e., weights in the policy model are randomly initialized), which requires lots of episodes to maximize the return. Inspired by recent advances in zero/few-shot learning for language models [13, 42], we pretrain our query model on a diverse set of PE tasks via *multi-task RL* across multiple episodes. The goal is to enhance the model’s query efficiency on a new PE task within a single episode.

Existing multi-task RL techniques [15, 17, 56] face two limitations in our problem. First, they require a shared action space for all tasks, while our PE tasks have specific action/query spaces. Second, they may experience the *negative transfer* issue, where training on some tasks negatively impacts others [45, 55]. To address the first limitation, we implement our query model as a Graph Neural Network (GNN), which can be generalized across diverse PE tasks with different query spaces. To mitigate the negative transfer issue, we first use domain knowledge to divide the PE task space into subspaces, each containing non-interfering tasks, and then pretrain a specialized query model for each subspace. Further details on the query model and its negative transfer mitigation are discussed in the following section.

4.3 Query Model

Our idea is to generate a query embedding (vector representation) for each query within the query space of the current abstract IAM configuration. This embedding is used to infer a probability distribution over the query space for query sampling/selection. To achieve this, we encode the current abstract IAM configuration into a graph where queries are represented as edges, and utilizes GNN to generate these edge embeddings. Note that the GNN’s capability to effectively process and generalize across various graph structures allows our query model to generate query embeddings for any arbitrary abstract IAM configurations. This enables us to pretrain our query model across diverse PE tasks. The following subsection details the graph representations, model architecture, and pretraining process.

4.3.1 The Graph Representation. In this section, we explain how we transform an abstract IAM configuration into a directed graph representation, which serves as the input for our GNN-based

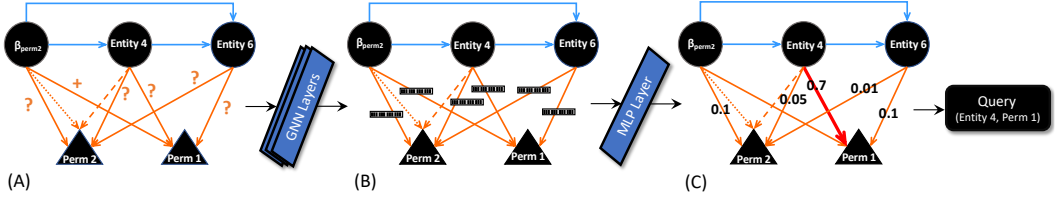


Fig. 7. The design and workflow of the query model.

query model. The nodes in the converted graph representation are generally classified into two types: entity nodes and permission nodes. Entity nodes are further classified into three sub-types: the pseudo entity type, untrusted entity type, and other entity type; permission nodes can be further classified into two sub-types: target permission type and Type-I permission type (there is no Type-II permission type, since all Type-II permissions are converted into Type-I permissions as introduced in Section 3.2.1). The directed edges in the graph are generally classified into two types, entity-entity type representing permission flows, and entity-permission type including three sub-types: (1) edges representing the permission assignments from an entity to one of its assigned permissions; (2) edges from a source entity of the permission flow in a Type-I permission to the corresponding Type-I permission; (3) edges from a sink entity of the permission flow in a Type-I permission to the corresponding Type-I permission. Note that each permission assignment edge in sub-type (1) with unknown abstract state $?$ also represents one query. The features of the nodes and edges include their corresponding types. In addition, the features of edges representing the permission flows and assignments also include their corresponding abstract values \hat{W} and \hat{A} , respectively. Figure 6 shows the input graph representation of the abstract IAM configurations shown in Figure 3b.

4.3.2 GNN-based Model Design. Given the graph representation of the abstract IAM configuration as the input, GNN-based query model first samples an entity-permission edge representing a permission assignment with $?$ abstract state in the input graph, based on the inferred probability distribution. Then, it outputs the corresponding query of the sampled permission assignment edge. The idea is to let the query model predict which permission assignment with the unknown state is critical for the PE detection.

Figure 7 illustrates the design and workflow of our GNN-based query model. Given a graph representation of an abstract IAM configuration, shown as the graph (A), five stacked Graph Attention Network named GATv2 layers [12] are first applied to generate the embedding of the permission assignment edges, shown as the graph (B). A Multi-Layer Perceptron (MLP) layer is then applied to predict the probability distribution over the query edges (permission assignment edges with $?$ abstract state), shown as the graph (C). Last, a query edge is sampled from the predicted probability distribution, which is converted into a query with the same corresponding entity and permission, as the output of the query model. For example, as shown in Figure 7, the edge from Entity 4 to Perm 1 is sampled since it has the highest probability. Thus, the corresponding query (Entity 4, Perm 1) is selected as the output of the query model.

4.3.3 Model Pretraining. To address the negative transfer issue mentioned in Section 4.2, our intuition is that PE tasks involving the same untrusted entity type are likely to share similar optimal query policies for detecting PEs. Therefore, they are unlikely to interfere with each other during model pretraining. Based on this intuition, we pretrain a query model on PE tasks with the same untrusted entity type. Specifically, given a set of pretraining tasks, we first divide them into groups

according to their untrusted entity types. For each group, we pretrain a distinct query model specialized for handling PE tasks with that specific untrusted entity type. This is achieved using RL with a sequential task scheduling strategy, where PE tasks in the group are randomly shuffled and sequentially used to optimize the query model over multiple episodes per task.

5 IAMVULGEN

Both our pretraining and evaluation require a large, diverse and challenging IAM PE task set. To our knowledge, the only publicly available IAM PE task set is IAM Vulnerable [1], which only includes 31 simple tasks. To remedy the lack of PE tasks, we introduce IAMVulGen, aiming to synthesize IAM PE tasks that are diverse and can mimic PEs in real-world scenarios.

Based on AWS’s official documentation [4–6] and recent studies on IAM PEs [20, 28, 30, 60], we identified 72 common entity types and 219 permission flow templates, giving rise to thousands of potential entities and millions of possible permissions. Consequently, IAMVulGen is able to generate IAM misconfigurations with any size up to the identified entity and permission space. In particular, IAMVulGen constructs each IAM PE task in two steps: 1) generate a concrete IAM misconfiguration; 2) generate the corresponding initial abstract IAM misconfiguration.

5.1 Concrete Misconfiguration Generation

To generate a concrete IAM misconfiguration with PE, IAMVulGen first randomly generates a concrete IAM configuration by creating the four components of a PFG $G = (E, F, \mathcal{A}, \mathcal{W})$:

- The entity space E is constructed based on 72 common entity types manually identified from AWS official service documentation [4–6], including user, user group, role, and 69 service types. IAMVulGen uniformly samples n ($n \in [1, 5]$ by default) entity types from the identified types. For each selected type, it generates m ($m \in [1, 20]$ by default) entities.
- The permission flow space F is created based on 219 *permission flow templates* manually extracted from AWS service authorization reference documentation [5] and studies on IAM PEs [20, 28, 30, 60]. The template identifies the type of each entity pair that has a permission flow. Given the generated entity space E , IAMVulGen adds a permission flow between each entity pair that has the identified type in a template.
- To build the permission assignment \mathcal{A} , the first step is to generate a permission space P including Type-I, Type-II, and target permissions. A Type-I permission is created for each generated permission flow to enable the flow. For the Type-II permission, three entity types (i.e., user, user group and role) are manually identified which can be directly assigned with a Type-I/target permission; for each entity with one of these types and each Type-I/target permission, IAMVulGen generates a Type-II permission for assigning the Type-I/target permission to the entity. For the target permission, based on AWS IAM security best practice documentation [6] and studies [20, 28, 30, 60], permissions which attackers usually target to obtain (e.g., the permission to access a sensitive S3 bucket) are manually identified. With the generated permission space, IAMVulGen creates the permission assignment component \mathcal{A} , by assigning each entity with γ_p ($\gamma_p = 20\%$ by default) of the permissions uniformly sampled from the permission space.
- For the flow state function \mathcal{W} , IAMVulGen sets the state of each permission flow to `true` with the probability of γ_w ($\gamma_w = 0.2$ by default) and to `false` with the probability of $1 - \gamma_w$. With the generated PFG, the fixed point iteration is performed to produce a concrete IAM configuration (as introduced in Section 3.1.3).

With the generated IAM configuration, an entity and a permission are uniformly selected from the configuration’s entity and permission spaces to be the untrusted entity and the target permission, respectively. Next, IAMVulGen utilizes four precise whitebox PE detectors to check if there exists a PE in the generated concrete IAM configuration. If at least one detector reports a PE,

the concrete misconfiguration is thus generated; otherwise, the process iterates by generating a new configuration. The applied four whitebox PE detectors include three state-of-the-art IAM PE detectors, namely Pacu [33], Cloudsplaining [47] and PMapper [21], and a whitebox variant of TAC which only applies the concrete IAM modeling to detect PEs, namely TAC-WB.

5.2 Initial Abstract Misconfiguration Generation

As introduced in Section 3.2.1, the initial abstract IAM configuration is generated with the pre-defined visible entities. Based on the created concrete misconfiguration, IAMVulGen creates the corresponding initial abstract IAM misconfiguration by uniformly sampling γ_v ($\gamma_v = 20\%$ by default) of entities in the concrete IAM misconfiguration as the visible entities.

6 IAMVULGEN

Both our pretraining and evaluation require a large, diverse and challenging IAM PE task set. To our knowledge, the only publicly available IAM PE task set is IAM Vulnerable [1], which only includes 31 simple tasks. To remedy the lack of PE tasks, we introduce IAMVulGen, aiming to synthesize IAM PE tasks that are diverse and can mimic PEs in real-world scenarios.

Based on AWS’s official documentation [4–6] and recent studies on IAM PEs [20, 28, 30, 60], we identified 72 common entity types and 219 permission flow templates, giving rise to thousands of potential entities and millions of possible permissions. Consequently, IAMVulGen is able to generate IAM misconfigurations with any size up to the identified entity and permission space. In particular, IAMVulGen constructs each IAM PE task in two steps: 1) generate a concrete IAM misconfiguration; 2) generate the corresponding initial abstract IAM misconfiguration.

6.1 Concrete Misconfiguration Generation

To generate a concrete IAM misconfiguration with PE, IAMVulGen first randomly generates a concrete IAM configuration by creating the four components of a PFG $G = (E, F, \mathcal{A}, \mathcal{W})$:

- The entity space E is constructed based on 72 common entity types manually identified from AWS official service documentation [4–6], including user, user group, role, and 69 service types. IAMVulGen uniformly samples n ($n \in [1, 5]$ by default) entity types from the identified types. For each selected type, it generates m ($m \in [1, 20]$ by default) entities.
- The permission flow space F is created based on 219 *permission flow templates* manually extracted from AWS service authorization reference documentation [5] and studies on IAM PEs [20, 28, 30, 60]. The template identifies the type of each entity pair that has a permission flow. Given the generated entity space E , IAMVulGen adds a permission flow between each entity pair that has the identified type in a template.
- To build the permission assignment \mathcal{A} , the first step is to generate a permission space P including Type-I, Type-II, and target permissions. A Type-I permission is created for each generated permission flow to enable the flow. For the Type-II permission, three entity types (i.e., user, user group and role) are manually identified which can be directly assigned with a Type-I/target permission; for each entity with one of these types and each Type-I/target permission, IAMVulGen generates a Type-II permission for assigning the Type-I/target permission to the entity. For the target permission, based on AWS IAM security best practice documentation [6] and studies [20, 28, 30, 60], permissions which attackers usually target to obtain (e.g., the permission to access a sensitive S3 bucket) are manually identified. With the generated permission space, IAMVulGen creates the permission assignment component \mathcal{A} , by assigning each entity with γ_p ($\gamma_p = 20\%$ by default) of the permissions uniformly sampled from the permission space.
- For the flow state function \mathcal{W} , IAMVulGen sets the state of each permission flow to `true` with the probability of γ_w ($\gamma_w = 0.2$ by default) and to `false` with the probability of $1 - \gamma_w$. With the

Task Set	Source	# Task	# Untrusted Entity Type	# Visible Entity			# Visible Perm Flow			# Permission		
				min	max	avg	min	max	avg	min	max	avg
Pretrain	IAMVulGen	2,000	51	2	34	15	2	274	48	6	313	67
Test-A	IAMVulGen	500	51	3	27	14	2	300	70	12	322	72
Test-B	IAM Vulnerable	31	2	1	3	2	0	6	2	3	12	7
Test-C	Security Startup	2	2	15	25	20	84	261	172	88	252	170

Table 1. Statistics of three PE task sets.

generated PFG, the fixed point iteration is performed to produce a concrete IAM configuration (as introduced in Section 3.1.3).

With the generated IAM configuration, an entity and a permission are uniformly selected from the configuration’s entity and permission spaces to be the untrusted entity and the target permission, respectively. Next, IAMVulGen utilizes four precise whitebox PE detectors to check if there exists a PE in the generated concrete IAM configuration. If at least one detector reports a PE, the concrete misconfiguration is thus generated; otherwise, the process iterates by generating a new configuration. The applied four whitebox PE detectors include three state-of-the-art IAM PE detectors, namely Pacu [33], Cloudsplaining [47] and PMapper [21], and a whitebox variant of TAC which only applies the concrete IAM modeling to detect PEs, namely TAC-WB.

6.2 Initial Abstract Misconfiguration Generation

As introduced in Section 3.2.1, the initial abstract IAM configuration is generated with the pre-defined visible entities. Based on the created concrete misconfiguration, IAMVulGen creates the corresponding initial abstract IAM misconfiguration by uniformly sampling γ_v ($\gamma_v = 20\%$ by default) of entities in the concrete IAM misconfiguration as the visible entities.

7 EVALUATION

7.1 Experimental Setup

7.1.1 Pretraining and Testing Task Sets. To pretrain TAC, we create an IAM PE task set called Pretrain, containing 2,000 tasks randomly generated by our task generator IAMVulGen under its default setting. To evaluate TAC, we create three testing task sets: 1) Test-A set consisting of 500 new tasks randomly generated by IAMVulGen under its default setting, and 2) Test-B set consisting of 31 tasks collected from public IAM PE benchmark set called IAM Vulnerable [1], and Test-C set consisting of two real-world misconfigurations with PEs collected from a US-based cloud security startup. Note that none of the three testing task sets overlap with the Pretrain set.

Table 1 shows the statistics of the generated task sets. The Pretrain task set includes diverse PE tasks with 51 untrusted entity types, having 2–34 visible entities, 2–274 visible permission flows, and 6–313 permissions. The Test-A task set has similar statistics. In contrast, Task-B set includes much smaller and less diverse tasks with only 2 untrusted entity types, 1–3 visible entities, 0–6 permission flows, and 3–12 permissions.

The Test-C task set includes two real-world misconfigurations, namely Real-1 and Real-2. Real-1 has 15 visible entities, 84 permission flows, and 88 permissions. Real-2 has 25 visible entities, 261 permission flows, and 252 permissions. Due to a data security protocol with the startup and its clients, we cannot disclose specific details. However, both misconfigurations involve at least one transitive PE with paths of at least five steps, presenting significant detection challenges within a limited query budget.

7.1.2 Customer Query Response Simulation. As introduced, TAC interacts with cloud customers in detecting IAM PEs. To evaluate TAC with hundreds of PE tasks, we build a customer query response simulator. Given an IAM PE task, the query response simulator randomly samples a set of queries

from the query space to serve as the ones that cloud customers accept to answer. Given a concrete IAM configuration and a query selected by TAC, the simulator automatically decides whether to accept the query based on the sampled query set, and gives the answer to the accepted query based on the concrete IAM configuration.

7.1.3 Baselines. Given the absence of publicly available greybox or blackbox IAM PE detectors, we take three state-of-the-art open-source whitebox PE detectors as our baselines, including Pacu [33], Cloudsplaining [47] and PMapper [21]. Besides, to understand the effectiveness of TAC’s IAM modeling, we also include the whitebox variant of TAC, namely TAC-WB, which only applies our concrete IAM modeling to detect PEs. In addition, to understand how the GNN-based RL helps to improve the performance of the query model, we build two greybox variants of TAC: one with a query model which randomly selects queries, namely TAC-RD; the other one with a query model trained by the state-of-the-art evolutionary algorithm called CMA-ES [22], namely TAC-EA. To understand how pretraining helps to improve the query model performance, we build another greybox variant of TAC, where the query model learns from scratch without pretraining (i.e., having the query model initialized with default model parameters by pytorch), namely TAC-NoPT.

7.1.4 Evaluation Metrics. To evaluate the effectiveness of TAC, we use the false negative rate (FNR) as the evaluation metric, which is defined as $FNR = \frac{|T|-|D|}{|T|}$ in our setting, where $|T|$ refers to the size of the whole task set T , and $|D|$ be the size of the task set $D \subseteq T$ where PEs are successfully identified by the detector. Note that we do not measure false positive rates, as all detectors in our experiments are *precise*. To evaluate the efficiency of TAC, we use the *query count* as our evaluation metric, which is the number of queries used to interact with the customer during the detection.

7.1.5 Query Budgets. In real-world scenarios, customers set the query budget based on their willingness to answer queries. The larger this budget is, the more information TAC obtains, increasing its chances of detecting PEs. For our experiments, we deliberately chose smaller query budgets to challenge TAC and assess its performance. In detail, for Test-A and Test-C task sets, we have 10 query budgets, which are set to 10, 20, 30, . . . , 100, respectively. Note that these query budgets are set much smaller than the maximum size of the query space (which is 8,448). For Test-B task set (the maximum size of the query space is 27), we have two query budgets which are set to 10 and 20, respectively.

7.1.6 Hyper-Parameter Settings. In the pretraining, each task is used to pretrain a query model in 20 episodes. In addition, the AdamW optimizer [36] with a learning rate of 10^{-4} is applied in both the pretraining and testing. To obtain reliable results, each experiment including the pretraining and testing is repeated 11 times.

7.2 Research Questions

We try to answer the following three research questions:

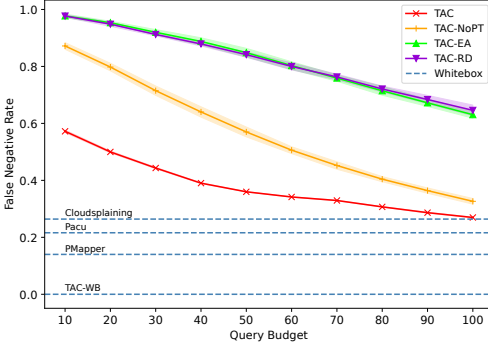
RQ1: How effective is our concrete IAM modeling?

RQ2: How effective is TAC in terms of false negative rate?

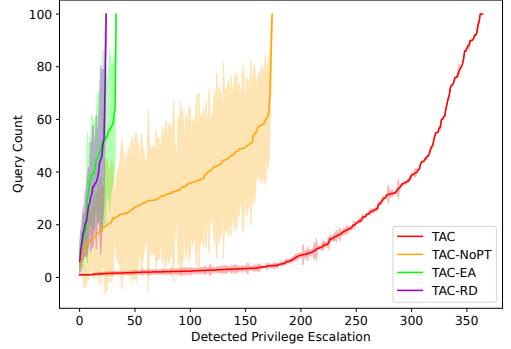
RQ3: How efficient is TAC in terms of query count?

7.3 Experimental Results

7.3.1 RQ1: Effectiveness of Concrete IAM Modeling. To empirically evaluate our concrete IAM modeling, we run all three whitebox baselines and TAC-WB on the task set Test-A, Test-B and Test-C. TAC-WB detects all PEs of the three task sets, achieving zero false negative rate. In contrast, on Test-A set, the false negative rates of PMapper, Pacu and Cloudsplaining are 12%, 20% and



(a) False negative rates of TAC and its three variants on Test-A across 10 different query budgets. For further comparisons, the false negative rates of the four whitebox baselines are also added, represented in four blue dashed lines.



(b) The query efficiency of TAC and its three greybox variants in detecting PE tasks in Test-A under the query budget of 100. Under the same query count, TAC consistently identifies more PEs than the three greybox variants.

Fig. 8. Evaluation results. Solid lines and their corresponding shadow regions refer to the mean and standard deviation of false negative rates or query counts over 11 repeated experiments, respectively.

26%, respectively; on Test-B set, the false negative rates of PMapper, Pacu and Cloudsplaining are 29%, 32% and 39%, respectively; On the Test-C set, PMapper, Pacu, and Cloudsplaining fail to detect both PEs, resulting in a 100% false negative rate. Upon manual inspection, we found that the false negative cases of pattern-based detectors, Pacu and Cloudsplaining, arose from the absence of relevant PE patterns; the false negative instances of the graph-based detector, PMapper, resulted from the limited expressiveness of their graph representations. *Overall, the impressively low false negative rates of TAC-WB underscore the significant benefits of our specific modeling approach.*

7.3.2 RQ2: Effectiveness of TAC. On Test-A set, Figure 8a illustrates the false negative rates of TAC compared to four whitebox baselines and its three greybox variants, across 10 different query budgets. We can observe that, as the query budget increases from 10 to 100, TAC’s false negative rate keeps decreasing significantly from 57% to 27%, and is always significantly lower than the false negative rates of its three greybox variants. Moreover, the standard deviation of TAC’s false negative rate is close to zero, indicating that TAC’s performance is apparently more stable than its three greybox variants. These results demonstrate that both GNN-based RL and the pretraining can significantly help improve the effectiveness of TAC. In comparison to the whitebox baselines, TAC’s false negative rate under a query budget of 100 is close to Cloudsplaining (which is 26%), and is only 6% and 14% higher than the false negatives than Pacu and PMapper, respectively. This already shows the significant effectiveness of TAC as a greybox detector, with limited access to partially queried information. Inspired by this promising result, we further increase the query budget of TAC to study the effectiveness of TAC under larger query budgets. As a result, TAC performs better than all three whitebox baselines when the query budget is increased to 258. This result shows the substantial superiority of our IAM modeling approach which considers a broader class of PEs than the three state-of-the-art whitebox baselines. *In general, results show that TAC exhibits competitive effectiveness on Test-A set, comparing to its greybox variants and state-of-the-art whitebox baselines.*

On Test-B set, TAC successfully detects 23 PEs within a query budget of 10, with a false negative rate of just 3%. Furthermore, TAC identifies all 31 PEs within a query budget of 20, which not only

outperforms the three state-of-the-art whitebox baselines, but also achieves the performance of TAC-WB. In comparison, the greybox variants of TAC detect between 17 and 22 PEs within a query budget of 10, resulting in a false negative rate ranging from 29% to 45%; they detect between 23 and 30 PEs within a query budget of 20, yielding a false negative rate ranging from 3% to 26%. On Test-C set, TAC successfully detects both PEs when the query budget is set to 60 or above. On the contrary, the greybox variants of TAC fail to detect both PEs across all query budgets. *In summary, TAC achieves the lowest false negative rate on both Test-B and Test-C sets.*

7.3.3 RQ3: Efficiency of TAC. To investigate how our proposed GNN-based RL with pretraining helps to improve the query efficiency, we compare TAC with its greybox variants in terms of query count. Figure 8b shows the query count of TAC and its greybox variants under the query budget of 100 on Test-A set. For a clear demonstration, we sort the detected PEs for each detector, based on the average query count derived from 11 repeated experiments in its ascending order.

We can observe that, for the same number of detected PEs, TAC consistently operates with a significantly smaller query count compared to its greybox variants; given the same query count, TAC consistently identifies many more PEs. Specifically, in comparison to TAC, TAC-NoPT only detects 175 PEs at an average query count that is 4.5 to 22.4 times greater than that of TAC, and TAC-NoPT exhibits substantially higher standard deviations. We can learn from the results that the pretraining is crucial for improving and stabilizing the query efficiency. In addition, TAC-EA detects merely 34 PEs at an average query between 8.2 to 61.1 times that of TAC. TAC-RD performs even worse than TAC-EA. The results show that our GNN-based RL approach substantially lowers the query count of TAC. *In sum, we can say that the GNN-based RL with pretraining plays an essential role in improving and stabilizing the query efficiency of TAC.*

8 RELATED WORK

IAM PE Detection and Modeling. For IAM PE detection, existing cloud security teams only focus on building whitebox cloud penetration testing tools. These tools can be classified into three kinds: *pattern-based* approach, *graph-based* approach and *reasoning-based* approach. For the pattern-based approach, Gietzen was the first to identify 21 typical IAM PE patterns[20]. Two whitebox detectors Pacu [33] and Cloudsplaining [47] select relevant PE patterns identified by Gietzen to discover IAM PEs. However, these tools do not support detecting *transitive PEs* (i.e., attackers gain sensitive permissions indirectly through intermediate entities) [2].

Graph-based approaches are proposed to mitigate this limitation. PMapper [21] models the authentication relation between users/roles (i.e., whether a user/role can be authenticated as another user/role through permissions) in an IAM configuration as a directed graph. With the graph modeling, PMapper detects a certain kind of transitive PEs by checking if a non-admin user/role can be authenticated as an admin user. AWSPX [34] applies similar graph modeling, and further visualizes the detected PEs. These approaches have two limitations: 1) the graph modeling considers only authentications between users/roles, ignoring possible PEs among other entity types (e.g., services) or caused by non-authentication strategies (e.g., changing the default version of an IAM policy [3]); 2) they ignore the fact that PEs can be realized by obtaining sensitive permissions from non-admin entities. TAC models the IAM configuration based on our defined permission flow graph which is more comprehensive for detecting PEs w.r.t. both admin and non-admin entities with broader entity types.

For reasoning-based approach, Ilia and Oded [53] recently employs SMT-based bounded model checking to formally verify if IAM configurations have PEs. While this approach represents IAM configurations with SMT formulas for whitebox detection, TAC represents IAM configurations as

abstract PFGs for greybox penetration testing. Unfortunately, by the time of the paper submission, this reasoning-based detector has not been made publicly available.

The modeling used in IAM PE detection can also be adapted for IAM PE repair. IAM-Deescalate[14] is the first approach for IAM PE repair, utilizing IAM modeling from PMapper[21]. Recently, IAMPERE [23], built on the IAM modeling of TAC, has shown significant improvements over IAM-Deescalate in both effectiveness and efficiency, highlighting the superiority of TAC’s IAM modeling.

Formal Methods for IAM. Besides IAM PE detection tools, there are IAM security tools using formal methods to address broader security issues. The AWS team has developed several formal verification tools for IAM, including ZELKOVA [10], Block Public Access [11], and Amazon Verified Permission [9]. These tools utilize SMT solvers to verify non-PE security and availability properties of IAM configurations, such as determining whether a user can access a resource. Eiers et al.[18, 19] introduced a quantitative IAM policy analysis framework based on model counting to identify and mitigate security risks associated with overly permissive IAM policies. Unlike these tools that rely on automated logical reasoning techniques, TAC models IAM configurations as permission flow graphs, enabling PE detection through a lightweight fixed-point iteration process without complex reasoning.

RL for Greybox Penetration Testing. RL has been extensively utilized to enhance greybox penetration testing. Existing tools [48–51, 54, 58] use the Partially Observable Markov Decision Process (POMDP) [38] to select attack operations based on partial network/system configurations. Our abstract IAM modeling enables TAC to frame the query decision problem as a classic Markov Decision Process, which can be optimized effectively and efficiently using advanced RL approaches. In contrast, optimizing POMDPs faces severe computational and statistical challenges [32, 35, 59], potentially affecting the performance of these testing techniques.

9 DISCUSSION

Applicability. Customers have a variety of options to simplify their query response procedures. They can utilize tools or services of the cloud provider to improve the efficiency of reviewing or assessing configurations. For instance, the official IAM Policy Simulator [7] is an excellent tool for shaping query responses. More specifically, to address a query about a permission assignment, customers can leverage the tool to simulate the entity applying the permission, avoiding the hassle of manual configuration analysis. Moreover, in the future, we plan to develop a light-weight open-source tool to provide a user-friendly GUI in aiding customers with their query response. This not only improves TAC’s applicability, but also allows customers to examine the source code of the tool to enhance the trustworthiness.

Although TAC is initially designed for AWS, it can be adapted to detect privilege escalations in other cloud platforms such as Google Cloud. This can be simply achieved by adding new permission flow templates based on other cloud’s official documentation. Moreover, the GNN and RL approach that TAC leverages to interact with humans in a semi-automated fashion can find broader applicability in security research, such as fuzzing, vulnerability repair, and privacy-centric machine learning, etc. For example, GNN-based RL can be employed in fuzzing to enhance seed scheduling and mutation operator selection, thereby boosting fuzzer’s capability of finding bugs. Furthermore, the interactive concept can be applied in efficient human-assisted fuzzing for enhancing the overall code coverage: GNN-based RL can be applied to intelligently identify critical and challenging constraints, and deliver to human experts who can then use their domain-specific knowledge to design high-quality test cases for these constraints.

Limitations. We identify three limitations of our approach. First, TAC requires customers to respond to queries manually. We have mitigated this by refining our query model with RL, reducing the

number of queries. Further, auxiliary tools can facilitate semi/fully automated responses. Second, without PEs present, TAC consumes its entire query budget before confirming their absence. An early-stopping mechanism, halting queries when PEs seem unlikely to appear, can address this. Third, the scarcity of real-world IAM misconfigurations makes it hard to assess how accurately IAMVulGen reflects actual scenarios. However, our permission flow templates are sourced from official documentation and manually verified, ensuring the validness and representativeness of the synthesized misconfigurations.

10 CONCLUSION

In this paper, we introduced the first greybox penetration testing approach, called TAC, designed for third-party cloud security services to detect IAM PEs due to misconfigurations. Unlike whitebox approaches that necessitate customers to anonymize their entire IAM configurations, TAC intelligently interacts with customers by selectively querying only the essential information required for detection. TAC relies on our comprehensive IAM modeling to identify a broad range of IAM PEs within partially visible IAM configurations and employs a GNN-based RL approach with pretraining to learn to detect PEs using as few queries as possible. To pretrain and assess TAC, we also proposed an IAM PE task generator named IAMVulGen. Experimental results illustrate that TAC is a promising approach, detecting IAM PEs with high query efficiency, and notably low false negative rates as competitive as those whitebox approaches.

REFERENCES

- [1] Seth Art. 2021. IAM Vulnerable - An AWS IAM Privilege Escalation Playground. <https://bishopfox.com/blog/aws-iam-privilege-escalation-playground>.
- [2] Seth Art. 2021. IAM Vulnerable - Assessing the AWS Assessment Tools. <https://bishopfox.com/blog/assessing-the-aws-assessment-tools>.
- [3] AWS. 2023. AWS IAM API Reference: SetDefaultPolicyVersion. https://docs.aws.amazon.com/IAM/latest/APIReference/API_SetDefaultPolicyVersion.html.
- [4] AWS. 2023. AWS Identity and Access Management (IAM). <https://aws.amazon.com/iam/>.
- [5] AWS. 2023. AWS Service Authorization Reference: Actions, resources, and condition keys for AWS services. https://docs.aws.amazon.com/pdfs/service-authorization/latest/reference/service-authorization.pdf#reference_policies_actions-resources-contextkeys.
- [6] AWS. 2023. Security best practices in IAM. <https://docs.aws.amazon.com/IAM/latest/UserGuide/best-practices.html>.
- [7] AWS. 2023. Testing IAM policies with the IAM policy simulator. https://docs.aws.amazon.com/IAM/latest/UserGuide/access_policies_testing-policies.html.
- [8] AWS. 2023. Using AWS IAM Access Analyzer. <https://docs.aws.amazon.com/IAM/latest/UserGuide/what-is-access-analyzer.html>.
- [9] AWS. 2023. What is Amazon Verified Permissions? <https://docs.aws.amazon.com/verifiedpermissions/latest/userguide/what-is-avp.html>.
- [10] John Backes, Pauline Bolignano, Byron Cook, Catherine Dodge, Andrew Gacek, Kasper Luckow, Neha Rungta, Oksana Tkachuk, and Carsten Varming. 2018. Semantic-based automated reasoning for AWS access policies using SMT. In *2018 Formal Methods in Computer Aided Design (FMCAD)*. IEEE, 1–9.
- [11] Malik Bouchet, Byron Cook, Bryant Cutler, Anna Druzkina, Andrew Gacek, Liana Hadarean, Ranjit Jhala, Brad Marshall, Dan Peebles, Neha Rungta, et al. 2020. Block public access: trust safety verification of access control policies. In *Proceedings of the 28th ACM Joint Meeting on European Software Engineering Conference and Symposium on the Foundations of Software Engineering*. 281–291.
- [12] Shaked Brody, Uri Alon, and Eran Yahav. 2021. How attentive are graph attention networks? *arXiv preprint arXiv:2105.14491* (2021).
- [13] Tom Brown, Benjamin Mann, Nick Ryder, Melanie Subbiah, Jared D Kaplan, Prafulla Dhariwal, Arvind Neelakantan, Pranav Shyam, Girish Sastry, Amanda Askell, et al. 2020. Language models are few-shot learners. *Advances in neural information processing systems* 33 (2020), 1877–1901.
- [14] Jay Chen. 2022. IAM-Deescalate: An Open Source Tool to Help Users Reduce the Risk of Privilege Escalation. <https://unit42.paloaltonetworks.com/iam-deescalate/>.

- [15] Myungsik Cho, Whyoung Jung, and Youngchul Sung. 2022. Multi-task reinforcement learning with task representation method. In *ICLR 2022 Workshop on Generalizable Policy Learning in Physical World*.
- [16] Cybersecurity Insiders. 2021. Cloud Security Report. <https://www.isc2.org/Landing/cloud-security-report>.
- [17] Carlo D’Eramo, Davide Tateo, Andrea Bonarini, Marcello Restelli, and Jan Peters. 2024. Sharing knowledge in multi-task deep reinforcement learning. *arXiv preprint arXiv:2401.09561* (2024).
- [18] William Eiers, Ganesh Sankaran, and Tevfik Bultan. 2023. Quantitative Policy Repair for Access Control on the Cloud. (2023).
- [19] William Eiers, Ganesh Sankaran, Albert Li, Emily O’Mahony, Benjamin Prince, and Tevfik Bultan. 2022. Quantifying permissiveness of access control policies. In *Proceedings of the 44th International Conference on Software Engineering*, 1805–1817.
- [20] Spencer Gietzen. 2018. AWS IAM Privilege Escalation – Methods and Mitigation. <https://rhinosecuritylabs.com/aws/aws-privilege-escalation-methods-mitigation/>.
- [21] NCC Group. 2023. Principal Mapper. <https://github.com/nccgroup/PMapper>.
- [22] Nikolaus Hansen. 2006. The CMA evolution strategy: a comparing review. *Towards a new evolutionary computation* (2006), 75–102.
- [23] Yang Hu, Wenxi Wang, Sarfraz Khurshid, Kenneth L McMillan, and Mohit Tiwari. 2023. Fixing Privilege Escalations in Cloud Access Control with MaxSAT and Graph Neural Networks. , 104–115 pages.
- [24] Orca Security Inc. 2024. Thrive Security in the Cloud. <https://orca.security/>.
- [25] Sysdig Inc. 2024. Cloud-Native vs. Third-Party Cloud Security Tools. <https://sysdig.com/learn-cloud-native/cloud-security/cloud-native-vs-third-party-cloud-security-tools/>.
- [26] Symmetry Systems Inc. 2024. Data Security Posture Management. <https://www.symmetry-systems.com/>.
- [27] Wiz Inc. 2024. Secure Everything You Build And Run in the Cloud. <https://go.wiz.io/>.
- [28] Eric Kedrosky. 2022. Achieving AWS Least Privilege: Understanding Privilege Escalation. <https://sonraisecurity.com/blog/common-methods-aws-privilege-escalation/>.
- [29] Shaharyar Khan, Ilya Kabanov, Yunke Hua, and Stuart Madnick. 2022. A systematic analysis of the capital one data breach: Critical lessons learned. *ACM Transactions on Privacy and Security* 26, 1 (2022), 1–29.
- [30] Gerben Kleijn. 2022. Well, That Escalated Quickly: Privilege Escalation in AWS. <https://bishopfox.com/blog/privilege-escalation-in-aws>.
- [31] Manjur Kolhar, Mosleh M Abu-Alhaj, and Saied M Abd El-atty. 2017. Cloud data auditing techniques with a focus on privacy and security. *IEEE Security & Privacy* 15, 1 (2017), 42–51.
- [32] Akshay Krishnamurthy, Alekh Agarwal, and John Langford. 2016. PAC reinforcement learning with rich observations. *Advances in Neural Information Processing Systems* 29 (2016).
- [33] Rhino Security Lab. 2022. Pacu: The Open Source AWS Exploitation Framework. <https://rhinosecuritylabs.com/aws/pacu-open-source-aws-exploitation-framework/>.
- [34] WithSecure Labs. 2022. A graph-based tool for visualizing effective access and resource relationships in AWS environments. <https://github.com/WithSecureLabs/awspx>.
- [35] Qinghua Liu, Praneeth Netrapalli, Csaba Szepesvari, and Chi Jin. 2023. Optimistic mle: A generic model-based algorithm for partially observable sequential decision making. In *Proceedings of the 55th Annual ACM Symposium on Theory of Computing*, 363–376.
- [36] Ilya Loshchilov and Frank Hutter. 2017. Decoupled weight decay regularization. *arXiv preprint arXiv:1711.05101* (2017).
- [37] Trend Micro. 2021. The Most Common Cloud Misconfigurations That Could Lead to Security Breaches. <https://www.trendmicro.com/vinfo/us/security/news/virtualization-and-cloud/the-most-common-cloud-misconfigurations-that-could-lead-to-security-breaches>.
- [38] George E Monahan. 1982. State of the art—a survey of partially observable Markov decision processes: theory, models, and algorithms. *Management science* 28, 1 (1982), 1–16.
- [39] Assaf Morag. 2021. Cloud Misconfigurations: The Hidden but Preventable Threat to Cloud Data. <https://www.infosecurity-magazine.com/opinions/cloud-misconfigurations-threat/>.
- [40] Capital One. 2022. Information on the Capital One Cyber Incident. <https://www.capitalone.com/digital/facts2019/>.
- [41] Momen Oqaily, Yosr Jarraya, Meisam Mohammady, Suryadipta Majumdar, Makan Pourzandi, Lingyu Wang, and Mourad Debbabi. 2019. SegGuard: segmentation-based anonymization of network data in clouds for privacy-preserving security auditing. *IEEE Transactions on Dependable and Secure Computing* 18, 5 (2019), 2486–2505.
- [42] Long Ouyang, Jeffrey Wu, Xu Jiang, Diogo Almeida, Carroll Wainwright, Pamela Mishkin, Chong Zhang, Sandhini Agarwal, Katarina Slama, Alex Ray, et al. 2022. Training language models to follow instructions with human feedback. *Advances in Neural Information Processing Systems* 35 (2022), 27730–27744.
- [43] Cedric Perneff. 2021. Research reveals that IAM is too often permissive and misconfigured. <https://www.techrepublic.com/article/research-iam-permissive-misconfigured/>.

- [44] Nathaniel Quist. 2021. Unit 42 Cloud Threat Report Update: Cloud Security Weakens as More Organizations Fail to Secure IAM. <https://unit42.paloaltonetworks.com/iam-misconfigurations/>.
- [45] Michael T Rosenstein, Zvika Marx, Leslie Pack Kaelbling, and Thomas G Dietterich. 2005. To transfer or not to transfer. In *NIPS 2005 workshop on transfer learning*, Vol. 898.
- [46] Jungwoo Ryoo, Syed Rizvi, William Aiken, and John Kissell. 2013. Cloud security auditing: challenges and emerging approaches. *IEEE Security & Privacy* 12, 6 (2013), 68–74.
- [47] Salesforce. 2022. Cloudsplaining. <https://cloudsplaining.readthedocs.io/en/latest/>.
- [48] Carlos Sarraute, Olivier Buffet, and Jörg Hoffmann. 2012. POMDPs make better hackers: Accounting for uncertainty in penetration testing. In *Proceedings of the AAAI Conference on Artificial Intelligence*, Vol. 26. 1816–1824.
- [49] Carlos Sarraute, Olivier Buffet, and Jörg Hoffmann. 2013. Penetration testing== POMDP solving? *arXiv preprint arXiv:1306.4714* (2013).
- [50] Jonathon Schwartz and Hanna Kurniawati. 2019. Autonomous penetration testing using reinforcement learning. *arXiv preprint arXiv:1905.05965* (2019).
- [51] Jonathon Schwartz, Hanna Kurniawati, and Edwin El-Mahassni. 2020. Pomdp+ information-decay: Incorporating defender’s behaviour in autonomous penetration testing. In *Proceedings of the International Conference on Automated Planning and Scheduling*, Vol. 30. 235–243.
- [52] Hemani Sehgal. 2021. Cloud Security Conundrum Debunked: Native Vs. Third-Party Tools. <https://www.horangi.com/blog/cloud-security-native-third-party-tools>.
- [53] Ilia Shevrin and Oded Margalit. 2023. Detecting {Multi-Step} {IAM} Attacks in {AWS} Environments via Model Checking. In *32nd USENIX Security Symposium (USENIX Security 23)*. 6025–6042.
- [54] Dorin Shmaryahu, Guy Shani, Joerg Hoffmann, and Marcel Steinmetz. 2018. Simulated penetration testing as contingent planning. In *Proceedings of the International Conference on Automated Planning and Scheduling*, Vol. 28. 241–249.
- [55] Trevor Standley, Amir Zamir, Dawn Chen, Leonidas Guibas, Jitendra Malik, and Silvio Savarese. 2020. Which tasks should be learned together in multi-task learning?. In *International conference on machine learning*. PMLR, 9120–9132.
- [56] Lingfeng Sun, Haichao Zhang, Wei Xu, and Masayoshi Tomizuka. 2022. Paco: Parameter-compositional multi-task reinforcement learning. *Advances in Neural Information Processing Systems* 35 (2022), 21495–21507.
- [57] Richard S Sutton and Andrew G Barto. 2020. *Reinforcement learning: An introduction*. MIT press.
- [58] Khuong Tran, Ashlesha Akella, Maxwell Standen, Junae Kim, David Bowman, Toby Richer, and Chin-Teng Lin. 2021. Deep hierarchical reinforcement agents for automated penetration testing. *arXiv preprint arXiv:2109.06449* (2021).
- [59] Nikos Vlassis, Michael L Littman, and David Barber. 2012. On the computational complexity of stochastic controller optimization in POMDPs. *ACM Transactions on Computation Theory (TOCT)* 4, 4 (2012), 1–8.
- [60] Xscaler. 2021. Anatomy of a Cloud Breach: How 100 Million Credit Card Numbers Were Exposed. <https://www.zscaler.com/resources/white-papers/capital-one-data-breach.pdf>.